

A New Magnetorheological Fluids Damper for Unmanned Aerial Vehicles

Open
Access

Ubaidillah^{1,*}, Bhre Wangsa Lenggana¹, Lovely Son², Fitriani Imaduddin¹, Purwadi Joko Widodo¹, Harjana³, Rumi Iqbal Doewes⁴

¹ Department of Mechanical Engineering, Faculty of Engineering, Universitas Sebelas Maret, 57126 Jebres, Surakarta, Indonesia

² Department of Mechanical Engineering, Faculty of Engineering, Universitas Andalas, 25163 Kota Padang, Sumatera Barat, Indonesia

³ Department of Physics, Faculty of Mathematics and Science, Universitas Sebelas Maret, Surakarta, 57126 Jebres, Surakarta, Indonesia

⁴ Department of Sport Education, Faculty of Physical Education, Universitas Sebelas Maret, Surakarta, 57126 Jebres, Surakarta, Indonesia

ARTICLE INFO

ABSTRACT

Article history:

Received 21 December 2019

Received in revised form 31 March 2020

Accepted 17 April 2020

Available online 5 July 2020

This case study proposes the development of damping technology using intelligent materials as working fluids for the landing gear of Unmanned Aerial Vehicles (UAV) during the landing process. The intelligent materials to be used are magnetorheological fluids (MRF), a liquid that has variable viscosity to magnetic fields. This intelligent material can improve the performance of the damping device by allowing it to have variable damping features through viscosity changing. The proposed UAV magnetorheological (MR) dampers design utilizes a magnetic valve that has an annular flow channel configuration with a 0.5 mm gap size equipped with an electromagnetic coil with adjustable current input. Both gap size and the current input selection affect the performance of the damping device. This study discusses the performance to reduce shock during the landing process. The performance is evaluated by analyzing the pressure drop and damping force produced by the device with changes in the current input variation. The numerical and simulation results show that the damping characteristics of the device could be adjusted by changing the current input to the electromagnet. The obtained results are then adjusted based on the needs of the UAV in landing purposes. The study proved that the device performance is suitable to absorb shock during the landing process of the UAV.

Keywords:

Unmanned aerial vehicle;
magnetorheological damper; landing
gear

Copyright © 2020 PENERBIT AKADEMIA BARU - All rights reserved

1. Introduction

Unmanned Aerial Vehicles (UAV) is a remote-controlled aircraft from a stationary or mobile command center. This vehicle does not have any human crew to drive the vehicle [1]. In general,

* Corresponding author.

E-mail address: ubaidillah_ft@staff.uns.ac.id

<https://doi.org/10.37934/arfmts.73.1.3545>

UAVs have some common features as normal aircraft. The landing gear, steering system, and shape of the vessel, they normally have a similar shape and same function to common aircraft [2].

One of the important components that are very useful for the UAV is a landing gear [3]. The basic function of the landing gear is similar with common shock absorber which is to absorb and dissipate the impact kinetic energy of the UAV's chassis or body frame during its landing process [4,5]. Besides absorbing the impact kinetic energy to reduce the vibrations transmitted to the UAV's main body, the landing gear has function to do maneuver during ground operations, such as takeoff, taxiing and landing [6]. The landing process is the most critical process because it involves a large impact energy transfer and the system must be operated stably under this condition. The original purpose of UAV was for monitoring and patrolling in military field [7]. Along with the needs and technological developments, the use of UAV technology has become favored by many application fields such as the management of crops, fisheries, forests and heavy-lift objects [8].

In order to absorb and dissipate the impact of kinetic energy during a landing process, several types of landing gear systems are applied. Oleo-pneumatic shock absorber system is the most common type that is used to absorb the impact of kinetic energy and reduce vibration. Oleo-pneumatic shock absorber system provides shock absorption effectively during landing and taxiing process [9].

The proposed study aims to discuss the ability of UAV landing gear performance with Oleo-pneumatic damper in heavy-lifting objects. The landing process of UAV must be balanced and stable. In order to achieve a balance and stability of the landing process, a damping device performance give a massive effect. In contrast to the general UAV damper that uses ordinary fluid, this study proposal uses magnetorheological (MR) fluid as the working fluid, it's called MR damper. As is well known that MR fluid is a fluid whose properties can change due to the influence of a magnetic field. MR fluid can generate field-dependent yield stresses with the supply of external magnetic fields or electric currents. The application of MR damper in the aerospace fields is relatively rare [10].

MR damper is a class of damping devices with a semi-active system. Semi-active systems have several advantages over other types of damping systems, namely passive and active systems. NASA already did research on active landing gear system in the 1970s. However, the active landing gear system was large, heavy and requires a massive amount of energy to power its sensors and actuators [10]. The semi-active system does not require high energy supply as active system. Moreover, the damping force of semi-active system can be controlled to adapt an external environment condition changes, whereas passive system cannot adapt to changes in the external environment conditions [11].

According to the research by NASA in the 1970s that the active landing gear system was large, heavy and requires high energy supply, this study is proposed with a new design semi-active MR damper that takes into consideration an optimal size, weight and energy supply by mathematical and simulation method.

2. Methodology

2.1 MR Fluids

The magnetorheological fluid is an intelligent fluid whose viscosity can change due to the influence of a magnetic field [12-14]. The viscosity changes by forming chains in direction of flux lines to the influence of a magnetic field as shown in Figure 1. In the absence of magnetic field, the MR fluids are similar to the base fluid [15,16]. MR fluids have been used in many applications due to its properties. One of the most popular applications that are being discussed is MR damper [17].

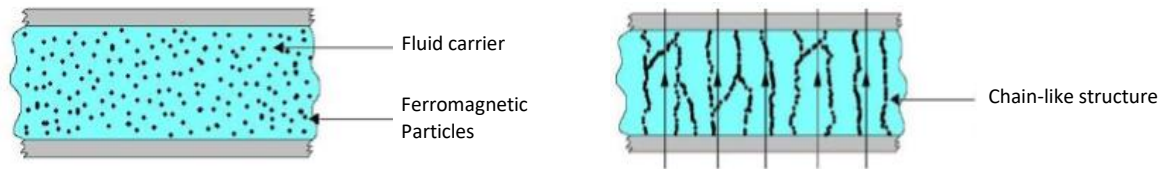


Fig. 1. Liquid to particles form chains in direction of flux line [15]

The working fluid that is used in this proposal is MR fluid 132-DG by Lord Corp. Table 1 shows the properties of the MRF-132DG.

Table 1
 Typical properties of mrf-132dg by lord corp

Typical Properties*	
Appearance	Dark Gray Liquid
Viscosity, Pa-s @ 40°C (104°F)	0.112 ± 0.02
Calculated as slope 800-1200 sec ⁻¹	
Density	
g/cm ³	2.95-3.15
(lb/gal)	(24.6-26.3)
Solids Content by Weight, %	80.98
Flash Point, °C (°F)	>150 (>302)
Operating Temperature, °C (°F)	-40 to +130 (-40 to +266)

2.2 MR Damper

An experimental setup configuration for the MR damper is established by the measurement of the MR valve [18], as shown in Figure 2. The details of MR valve are shown in Figure 3. The MR damper has 30 mm bore size, 69.5 mm stroke length and 12.5 mm rod size. The MR valve has an annular configuration with 0.5 mm gap size. The gap size has been adjusted according to calculations to achieve optimal damping forces and ease of manufacturing processes. The MR valve is divided into four main components with different materials, as shown in Figure 3. This aims to optimize the direction of magnetic flux. The flux lines can be directed through the flux route determination process by combining higher permeability materials (magnetic materials) and the materials with lower permeability (non-magnetic materials) in such a way so that the magnetic fluxes penetrate the MR fluid channel. The magnetic circuit design of MR application usually uses penetration of magnetic fluxes in the perpendicular direction to the direction of fluid flow [19]. Soft magnetic material is used to fabricate the bobbin and cover. This soft magnetic material is selected for the purpose of attracting the magnetic flux. On the other hand, both of the casings are fabricated with non-magnetic material. This non-magnetic material aims to limit and deflect the direction of magnetic flux. So that the direction of magnetic flux does not become disorganized. The coil uses 28 AWG copper wire. According to the Farnell datasheets, this copper wire has part number ECW0.315 with 0.315 mm nominal conductor diameter and 0.219 Ω/m at 20°C nominal electrical resistance. The wire through along the path on the drilled rod.

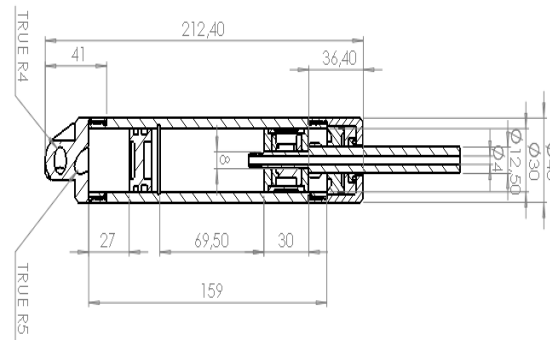


Fig. 2. The full Assembly MR damper

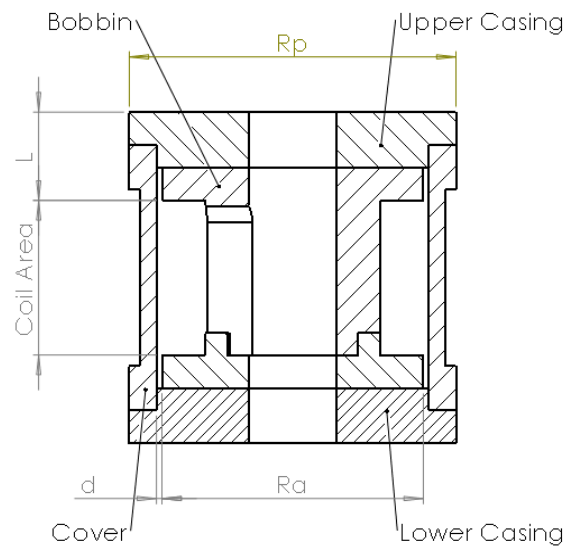


Fig. 3. Details of MR valve

MR valve that is proposed in this study has several parameter definitions as shown in Table 2. This MR valve has 16 mm effective area. The effective area is the area of the annular path gap that is subject to the influence of a magnetic field so that the fluid responds to the magnetic field which causes a change in its viscosity. The change of the viscosity results in an increase in pressure drop in the gap of the fluid path. The area of the magnetic field and the direction of magnetic flux on the MR valve can be simulated by Finite Element Method Magnetics (FEMM).

Table 2

The parameters data of the mr valve design

Parameters	Descriptions	Units	Value
η (MRF132DG)	Fluid viscosity	Pa s	0.112
d	Annular gap	mm	0.5
L	Annular channel length	mm	8
$L_e = 2 \times L$	Effective annular channel length	mm	16
R_a	Annular radius gap	mm	24
R_p	Piston radius	mm	30

2.3 Finite Element Method Magnetic Simulation

Finite Element Method Magnetic Simulation (FEMM) is used to simulate the MR valve design. The design that is simulated is 2D design with axisymmetric problem. FEMM simulation result the

magnetic flux density which is used to calculate the pressure drop in on-state condition. The on-state condition is the condition when the coil of the MR valve obtains an input of electric current. Figure 4 shows the result of FEMM simulation. By the simulation, magnetic flux densities on each electric currents input are obtained. Then, those values are used to calculate the yield stress of the fluid with Eq. (1) [20].

$$\begin{aligned} \tau_y(B) &= -58.92B^3 + 74.66B^2 + 35.74B - 3.387, \text{ for } \tau_y(B) > 0 \\ \tau_y(B) &= 0, \text{ for } \tau_y(B) \leq 0 \end{aligned} \quad (1)$$

where B is the magnetic flux density (Tesla) and τ_y is the yield stress of the fluid.

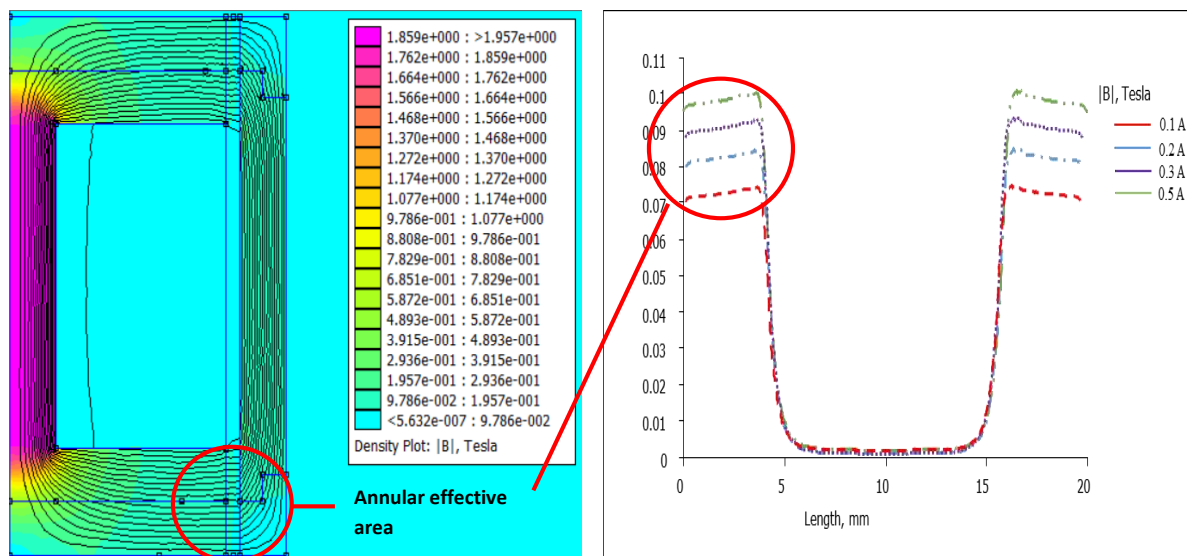


Fig. 4. FEMM simulation results

This magnetic flux density is affected by the properties of the fluid, number of coil turns and the varied current input of the MR valve coil. This MR valve design uses 350 number of coil turns with four varied current inputs, 0.1, 0.2, 0.3 and 0.5 Ampere for the peak varied current input. The result of magnetic flux density in each current input is 0.07, 0.08, 0.088, and 0.097 Tesla as shown in Figure 4. For this MR valve design, the result shows that between all of the varied current inputs, the peak magnetic flux density value is reached in 0.5 A with 0.097 Tesla. Then, the magnetic density value results are used to predict pressure drops for on-state conditions.

2.4 Analytical Model

The pressure drop is predicted in two conditions, those conditions are the conditions when the coil is not given an electromagnet current (off-state) and the condition of the coil is given an electromagnet current (on-state). Both of those conditions have each equation to be calculated. Eq. (2)-(3) expressed for off-state and on-state condition [21].

$$\Delta P_{viscous} = \frac{6\eta QL}{\pi d^3 R} \quad (2)$$

$$\Delta P_{yield} = \frac{c\tau(B)L}{d} \quad (3)$$

$\Delta P_{viscous}$ is the equation for the off-state condition. In this condition shows that viscous pressure drop ($\Delta P_{viscous}$) proportionally relates to the fluid viscosity (η), flow rate of the fluid (Q) and annular channel length (L), inverse to the radius of the annular channel (R_a) and cubically inverse to the gap of the annular channel (d). Then ΔP_{yield} is the equation for on-state condition. This yield pressure drop (ΔP_{yield}) is proportional to the field-dependent yield stress value ($\tau_y(B)$), flow-velocity profile coefficient (c) and annular channel length but inverse to the gap of the annular channel. The coefficient c in yield pressure drop is obtained by calculating the ratio between field-dependent and viscous pressure drop using approximation function in the following Eq. (4) [20].

$$c = 2.07 + \frac{12Q\eta}{12Q\eta + 0.8\pi R d^2 \tau(B)} \quad (4)$$

In order to find out the total pressure drop of the MR valve, the viscous and yield pressure drop obtained from Eq. (2) and Eq. (3) are summed. The total pressure drop can be expressed in Eq. (5) below [19].

$$\Delta P = \Delta P_{viscous} + \Delta P_{yield} \quad (5)$$

In order to predict the ability of device applications in landing processes, the damping force (F_d) must be predicted [22]. The generated total pressure drop from Eq. (5), then used to predict the performance of damping force the MR damper that can be expressed in Eq. (6). Eq. (6) shows that the damping force is proportional to the total pressure drop and the area of the piston valve (A_p). Eq. (7) is used to calculate the area of the piston valve [23,24].

$$F_d = \Delta P \times A_p \quad (6)$$

$$A_p = \pi R_p^2 \quad (7)$$

3. Results

The discussion of this study is presented in the performance of the MR valve generated pressure drop and the performance of the damping characteristics of the UAV damper. The MR valve section will discuss the variations of electromagnet current and the variation of piston speed that affect to the performance of the pressure drop [25]. Meanwhile, in the MR damper section will discuss the performance of MR valve is used to predict the performance of the UAV damper in generating adjustable damping force.

3.1 Pressure Drop Prediction

The pressure drop prediction can be used to predict the performance of the MR valve. As in Eq. (5), the total pressure drop is obtained by the addition between viscous (off-state) and yield (on-state) pressure drop [26]. The result of the pressure drop in the off-state condition that is variated to the piston speed is shown in Figure 5. The result shows that the pressure drop of the off-state condition increases to the piston speed variation. This is related to Eq. (2) which shows that the pressure drop is proportional to the flow rate of the fluid. The negative value of the piston speed is the value for extended or rebound piston position and the positive value is the value for compressed piston position. According to the result, the compressed pressure drop value is greater than the extended pressure drop. It is occurred because of the differences between the area compressed and

extended position. The piston rod makes the area of extended position is smaller than the compressed position.

The results of the pressure drop for the compressed position in varied piston speed reach 0.08 MPa with 0.1 m/s piston speed and 0.16 MPa with 0.2 m/s piston speed. The pressure drop results for the extended position with the same variation piston speed reach 0.06 MPa with 0.1 m/s and 0.13 MPa with 0.2 m/s piston speed.

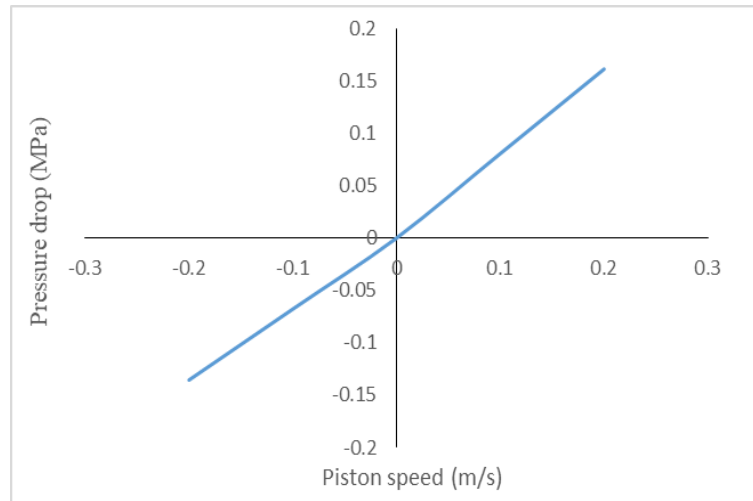


Fig. 5. Off-state pressure drop result

Meanwhile, the on-state pressure drop condition can be calculated with Eq. (3). Figure 6 shows the result of the on-state pressure drop prediction in 0.1, 0.2, 0.3 and 0.5 Amperes DC current input. The result of the peak on-state pressure drop reaches in 0.53 MPa with 0.5 A current input.

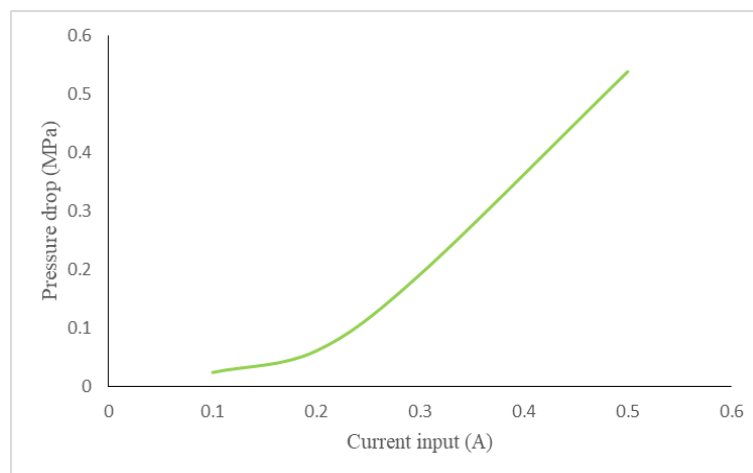


Fig. 6. On-state pressure drop result

The generated off-state and on-state pressure drop are used to predict the performance of the MR valve by total pressure drop. As in Eq. (5), the total pressure drop can be calculated. Figure 7 shows the total pressure drop values on each position with 0.1 and 0.2 m/s piston speed and the variation of the current input. The results show that the variations of current input and piston speed affect the pressure drop value. According to the results, increasing a piston speed results in increased pressure drop. This is caused by the pressure drop equation in viscous condition (off-state) directly proportional to the flow rate of the fluid, where the flow rate is obtained from the following equation.

$$Q = V_p \times A_p \tag{8}$$

where, V_p is the piston speed (m/s) and A_p is the area of the piston (m²).

From the off-state condition that can be called with the passive system, the increasing pressure drop to the effect of current input variations is very significant. The peak off-state pressure drop only reaches 0.16 MPa with 0.2 m/s in the compressed position and 0.13 MPa with 0.2 m/s in the extended position. Meanwhile, the peak of total pressure drop value that is affected by 0.5 A current input reaches 0.69 MPa with the same piston speed for the compressed position and 0.67 MPa for the extended position. The result of 0.1 m/s piston speed variation shows that in the compressed position, the total pressure drop generates 0.61 MPa with 0.5 A. The extended position with the same piston speed and current input generates 0.60 MPa.

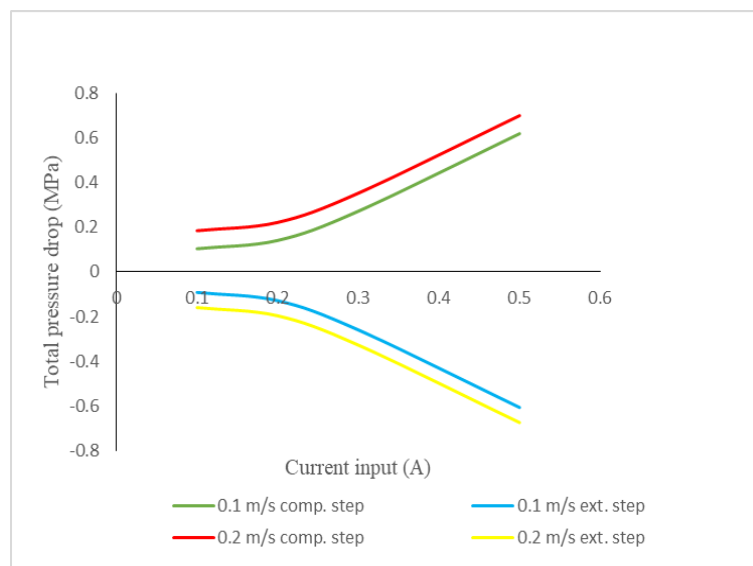


Fig. 7. Total pressure drop vs. current input

3.2 Damping Force Prediction

Since the total pressure drop value is calculated, the damping force can be predicted with Eq. (6). The damping force value results are used to predict the performance of the MR damper. Figure 8 shows the result of the damping force prediction versus piston speed with the variations of electromagnet current input. As in Figure 8, the damping force on each current input variations and off-state condition shows that its performance increases to the increase in piston speed value. It is in accordance with Eq. (6) that the damping force value is directly proportional to the increase in the value of the pressure drop which relates to the piston speed as mentioned in Eq. (2), Eq. (4) and Eq. (8). The piston speed is directly proportional to the flow rate and the flow rate is directly proportional to the viscous pressure drop [22]. Thus, the damping force will increase in the increase of the piston speed [25].

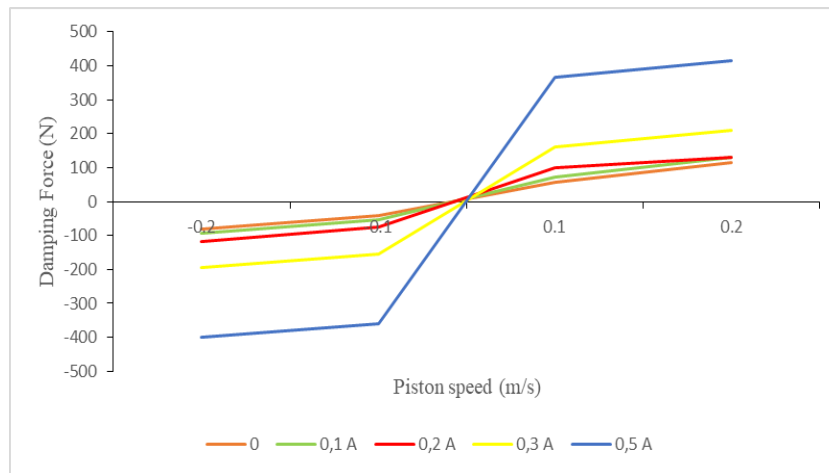


Fig. 8. Damping force prediction result

The results of the damping force prediction are shown in Table 3. The peak value of the damping force in a compressed position with 0.1 m/s is 367.2 N and 415.0 N for 0.2 m/s piston speed. The peak value of the damping force in extended or rebound position with 0.1 m/s is 359.5 N and 399.7 N for 0.2 m/s piston speed. The negative values in Table 3 mean that the piston valve is in an extended or rebound position. An extended position generates smaller results than compressed position. It is caused by the piston rod, so the area of the piston valve must be subtracted with the area of the piston rod. Table 3 shows the damping force result with the variations of electromagnet current inputs and piston speeds for compressed and extended position.

Table 3
 The results of the pressure drop prediction

F_d (N)	I (A)					
	0	0.1	0.2	0.3	0.5	
V (m/s)	0.1	56.9	73.6	99.7	161.4	367.2
	0.2	113.9	130.6	131.6	209.3	415.0
	-0.1	-40.2	-54.2	-76.1	-153.7	-359.5
	-0.2	-80.4	-94.4	-116.3	-193.9	-399.7

4. Conclusions

The study of the magnetorheological damper for Unmanned Aerial Vehicle (UAV) using simulation and analytical method has been presented. The design of this MR damper is used for the landing process in heavy lifting UAV. The result of the simulation and analytical study show that MR fluid can change its properties based on performance prediction. Then, the performance of MR damper can be predicted by calculating the pressure drop of the MR valve on the off-state and on-state condition. The prediction values for off-state, on-state and total pressure drop increase to the increase in piston speed and electromagnet current input variations. The prediction value for total pressure drop with 0.5 A current input increases to 0.69 MPa from 0.16 MPa in off-state condition. The results of the damping force increase directly proportional to the total pressure drop in each piston speed variations. The peak damping force value is reached in 0.5 A electromagnet current input with 0.2 m/s on compressed position.

Acknowledgement

This research was financially supported by Hibah Penelitian Pengembangan Hasil Riset dan Inovasi 2020, Universitas Sebelas Maret.

References

- [1] Son, Lovely, Mulyadi Bur, and Meifal Rusli. "A new concept for UAV landing gear shock vibration control using pre-straining spring momentum exchange impact damper." *Journal of Vibration and Control* 24, no. 8 (2018): 1455-1468.
<https://doi.org/10.1177/1077546316661470>
- [2] Skorupka, Zbigniew, Wojciech Kowalski, and Rafal Kajka. "Electrically Driven And Controlled Landing Gear For UAV Up To 100kg Of Take Off Mass." In *ECMS*, pp. 117-121. 2010.
<https://doi.org/10.7148/2010-0117-0121>
- [3] Matta, Anil Kumar, G. Vijay Kumar and R. Vijay Kumar. "Design Optimisation Of Landing Gear's Leg For An Un-Manned Aerial Vehicle." *International Journal of Engineering Research and Applications (IJERA)* 2, no. 4 (2012): 2069-2075.
- [4] Akhilesh Jha. "Landing gear layout design for unmanned aerial vehicle." *14th National Conference on Machines and Mechanisms (NaCoMM09)* (2009): 471-476.
- [5] Asthana, Chandra B., and Rama B. Bhat. "A Novel Design of Landing Gear Oleo Strut Damper Using MR Fluid for Aircraft and UAV's." In *Applied Mechanics and Materials*, vol. 225, pp. 275-280. Trans Tech Publications Ltd, 2012.
<https://doi.org/10.4028/www.scientific.net/AMM.225.275>
- [6] Li, Zhenming, Mingjie Lao, Swee King Phang, Mohamed Redhwan Abdul Hamid, Kok Zuea Tang, and Feng Lin. "Development and Design Methodology of an Anti-Vibration System on Micro-UAVs." In *International Micro Air Vehicle Conference and Flight Competition (IMAV)*, pp. 223-228. 2017.
- [7] Berie, Habitamu Taddese, and Ingunn Burud. "Application of unmanned aerial vehicles in earth resources monitoring: focus on evaluating potentials for forest monitoring in Ethiopia." *European Journal of Remote Sensing* 51, no. 1 (2018): 326-335.
<https://doi.org/10.1080/22797254.2018.1432993>
- [8] Suprpto, Bhakti Yudho, M. Ary Heryanto, Herwin Suprijono, Jemie Muliadi, and Benyamin Kusumoputro. "Design and development of heavy-lift hexacopter for heavy payload." In *2017 International Seminar on Application for Technology of Information and Communication (iSemantic)*, pp. 242-247. IEEE, 2017.
<https://doi.org/10.1109/ISEMANTIC.2017.8251877>
- [9] Kumar, J. Sri Ram. "Design of landing gear retraction system for UAV's." *Journal of Basic and Applied Engineering Research* 1, no. 3 (2014): 64-67.
- [10] Han, Chulhee, Bo-Gyu Kim, and Seung-Bok Choi. "Design of a new magnetorheological damper based on passive oleo-pneumatic landing gear." *Journal of Aircraft* 55, no. 6 (2018): 2510-2520.
<https://doi.org/10.2514/1.C034996>
- [11] Ahamed, Raju, Md Meftahul Ferdous, and Yancheng Li. "Advancement in energy harvesting magneto-rheological fluid damper: A review." *Korea-Australia Rheology Journal* 28, no. 4 (2016): 355-379.
<https://doi.org/10.1007/s13367-016-0035-2>
- [12] Kciuk, S., R. Turczyn, and M. Kciuk. "Experimental and numerical studies of MR damper with prototype magnetorheological fluid." *Journal of Achievements in Materials and Manufacturing Engineering* 39, no. 1 (2010): 52-59.
- [13] Pokaad, Alif Zulfakar Bin, Khisbullah Hudha, and Mohd Zakaria Bin Mohamad Nasir. "Simulation and experimental studies on the behaviour of a magnetorheological damper under impact loading." *International Journal of Structural Engineering* 2, no. 2 (2011): 164-187.
- [14] Sabino, Ubaidillah, Khisbullah Hudha, and Hishamuddin Jamaluddin. "Simulation and experimental evaluation on a skyhook policy-based fuzzy logic control for semi-active suspension system." *International Journal of Structural Engineering* 2, no. 3 (2011): 243-272.
<https://doi.org/10.1504/IJSTRUCTE.2011.040783>
- [15] Gadekar, Pranav, V. S. Kanthale, and N. D. Khaire. "Magnetorheological fluid and its applications." *International Journal of Current Engineering and Technology Special Issue* 7 (2017): 32-37.
- [16] Han, Chulhee, Bo-Gyu Kim, Byung-Hyuk Kang, and Seung-Bok Choi. "Effects of magnetic core parameters on landing stability and efficiency of magnetorheological damper-based landing gear system." *Journal of Intelligent Material Systems and Structures* 31, no. 2 (2020): 198-208.
<https://doi.org/10.1177/1045389X19862639>

- [17] Han, Chulhee, Byung-Hyuk Kang, Seung-Bok Choi, Jun Mo Tak, and Jai-Hyuk Hwang. "Control of Landing Efficiency of an Aircraft Landing Gear System With Magnetorheological Dampers." *Journal of Aircraft* 56, no. 5 (2019): 1980-1986.
<https://doi.org/10.2514/1.C035298>
- [18] Saleh, Muftah, Ramin Sedaghati, and Rama Bhat. "Crashworthiness Study of Helicopter Skid Landing Gear System Equipped With a Magnetorheological Energy Absorber." In *ASME 2017 Conference on Smart Materials, Adaptive Structures and Intelligent Systems*. American Society of Mechanical Engineers Digital Collection, 2017.
<https://doi.org/10.1115/SMASIS2017-3755>
- [19] Lee, Tae-Hoon, Byung-Hyuk Kang, and Seung-Bok Choi. "A quasi-static model for the pinch mode analysis of a magnetorheological fluid flow with an experimental validation." *Mechanical Systems and Signal Processing* 134 (2019): 106308.
<https://doi.org/10.1016/j.ymssp.2019.106308>
- [20] Patel, Dipal M., and Ramesh V. Upadhyay. "Testing and Evaluation of Linear Shear Mode Magnetorheological (MR) Damper Based on Rheological Properties of MR Fluid." *Journal of Testing and Evaluation* 48, no. 5 (2020).
<https://doi.org/10.1520/JTE20180030>
- [21] Powell, Louise A. Ahur , Young T. Choi, Wei Hu, and Norman M. Wereley. "Nonlinear modeling of adaptive magnetorheological landing gear dampers under impact conditions." *Smart Materials and Structures* 25, no. 11 (2016): 115011.
<https://doi.org/10.1088/0964-1726/25/11/115011>
- [22] Sabino, Ubaidillah, Khisbullah Hudha, Faizul Akmar, and A. Kadir. "Modelling, characterisation and force tracking control of a magnetorheological damper under harmonic excitation." *International Journal of Modeling Identification and Control* 13, no. 1/2 (2011): 9-21.
<https://doi.org/10.1504/IJMIC.2011.040485>
- [23] Weber, Felix, Hans Distl, Sebastian Fischer, and Christian Braun. "MR damper controlled vibration absorber for enhanced mitigation of harmonic vibrations." In *Actuators*, vol. 5, no. 4, p. 27. Multidisciplinary Digital Publishing Institute, 2016.
<https://doi.org/10.3390/act5040027>
- [24] Mikułowski, Grzegorz, and Łukasz Jankowski. "Adaptive landing gear: optimum control strategy and potential for improvement." *Shock and Vibration* 16, no. 2 (2009): 175-194.
<https://doi.org/10.1155/2009/732803>
- [25] Unuh, M. H., P. Muhamad, H. M. Y. Norfazrina, M. A. Ismail, and Z. Tanasta. "Study of Magnetic Flux and Shear Stress of OEM Damper featuring MR Fluid." *Journal of Advanced Research in Applied Mechanics* 41, no. 1 (2018): 9-15.
- [26] Choi, H. J., S. A. Mazlan, and Fitriani Imaduddin. "Fabrication and viscoelastic characteristics of waste tire rubber based magnetorheological elastomer." *Smart Materials and Structures* 25, no. 11 (2016): 115026.
<https://doi.org/10.1088/0964-1726/25/11/115026>